RESEARCH ARTICLE

Synthesis and characterization of zeolite NaX from Bangka Belitung Kaolin as alternative precursor

Vita Nur Iftitahiyah [a], Didik Prasetyoko [a, *], Hadi Nur [b], Hasliza Bahruji [c], Hartati [d]

[a] *Department of Chemistry, Faculty of science, Institut Teknologi Sepuluh Nopember (ITS), Kampus ITS Sukolilo, Surabaya 60111, Indonesia*
[b] *Ibnu Sina Institute for Scientific and Industrial Research, Universiti Teknologi Malaysia, 81310 UTM Skudai, Johor, Malaysia*
[c] *Cardiff Catalysis Institute, Cardiff University, CF10 3AT Cardiff United Kingdom*
[d] *Department of Chemistry, Faculty of Science and Technology, Universitas Airlangga, Kampus UNAIR, Surabaya 60115, Indonesia*
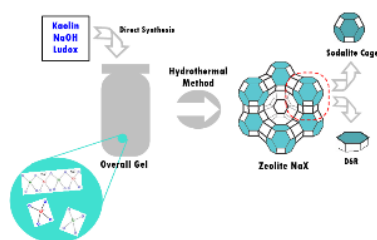
* *Corresponding author: didikp@chem.its.ac.id*

Graphical abstract

Abstract

The potential use of kaolin as silica and alumina precursor for the synthesis of zeolite NaX was investigated in this study. The synthesis involved three steps of reactions; the preparation of seed gel, the formation of feedstock gel using kaolin and the combination of overall gel followed by hydrothermal treatment at 105°C for 12 hours. Analysis using X-ray Diffraction (XRD) method indicated the transformation of kaolin into pure phase zeolite NaX with a small amount of kaolin was still visible. Detail microscopic analysis showed the morphology of zeolite X consisted of octahedral particles with a crystallite diameter of 20-30 μm. Analysis of surface acidity using pyridine as probe molecule indicated the zeolite X has high Brønsted acidity with 0.181 mmol/g of acid sites, significantly higher than Lewis acidity ~0.053 mmol/g. The N_2 adsorption-desorption measurement indicated a type IV material with both microporous and mesoporous structures with an average pore size of 1.47 nm for micropore and 3.41 nm for mesoporous.

Keywords: Kaolin, zeolite NaX, porous materials, hydrothermal method

INTRODUCTION

Zeolite consists of four connected AlO_4 and SiO_4 tetrahedrons connected via oxygen to form porous aluminosilicates framework. The intracrystalline channel in the zeolite framework is occupied with water molecule and cation to neutralise the negative charge of AlO_4. The mobility of the cation and the flexibility of the size, shape and pore structure of the zeolite allows modification to accommodate catalytic desire. Zeolite is commonly produced from hydrogels aluminate and sodium silicate, however, production of zeolite from alternative silica and alumina source such as bagasse fly ash [1] [2], rice hush ash [3] and kaolin [4] have received considerable attention since the past few decades. Kaolin is naturally occurring minerals that abundantly available in Indonesia particularly in south Sumatra, Bangka Belitung and Java island. Kaolin from Bangka Belitung has low iron and titanium content but rich with silica (54.9 wt.%) and alumina (36 wt.%). Studies were previously carried out for the synthesis of zeolite X using kaolin originated from Bulgaria [5] and also the synthesis of zeolite Y from natural kaolin [6], kaolin obtained from China [7] and Iran [8]. Kaolin is an ideal alternative candidate to replace commercial silica and alumina precursors due to a high level of silica and alumina with relatively low iron content. The use of kaolin as raw material for the synthesis of zeolite offers an alternative economical route by utilising naturally abundant resources rather than commercially available chemical.

The aim to synthesis zeolite NaX is due to its unique three-dimensional pore structure and surface acidity that can be utilised as a solid acid catalyst [9], ion exchanger [10], and adsorbent. Zeolite NaX belongs to faujasite family that composes of sodalite cage with 6-rings (D6R) to form hexagonal framework.

Studies that were carried out on the synthesis of zeolite X from kaolin required acid or base leaching treatment to reduce its resistance towards chemical transformation to zeolite [11]. Kaolin also required thermal treatment at high temperature ~ 700–900°C to form amorphous metakaolin before it can be used for zeolite synthesize [12]. The additional pre-treatment process has an indirect effect on the production cost and also detrimental to the environment i.e., production of greenhouse gases.

Here we investigate the potential of kaolin as alternative silica and alumina precursors without the need for pre-treatment to produce zeolite NaX via hydrothermal method. The physical properties of zeolite X were analysed using XRD, SEM, FTIR and N_2-gas adsorption-desorption methods to obtain its crystal morphology, framework structure, pore structure and surface acidity.

EXPERIMENTAL

Materials

Kaolin from Bangka Belitung contained 36 wt.% Al_2O_3, 54.9 wt.% SiO_2, 3.34 wt.% Fe_2O_3 and 1.88 wt.% K_2O. The materials used in the synthesis were sodium hydroxide (99 wt.% NaOH Merck), sodium aluminate (53 wt.% $NaAlO_2$ Merck), silica colloidal (LUDOX) (30 wt.% SiO_2 and 70 wt.% H_2O Merck), ammonium acetate (Merck) for ion exchanged and acidity characterization. Demineralized water was used for cleaning and chemical preparation.

Synthesis of zeolite NaX

Bangka Belitung kaolin used in this study was obtained from Bangka Belitung (Sumatra, Indonesia). Chemical and mineralogical composition of the received kaolin is listed in Table 1. The as-received kaolin contains a low level of metal oxide impurities with Si to Al molar ratio of 1.53. Kaolin was used for the synthesis of zeolite X without prior pretreatment. The mixture kaolin and other precursors were

dissolved in NaOH solution to produce amorphous Si and Al gel mixture which was then used for the hydrothermal synthesis of zeolite X.

The synthesis of zeolite NaX was carried out following three steps; the preparation of seed gel, the production feedstock gel and the mixing of seed and feedstock gels to produce an overall gel. The seed gel ($Al_2O_3.4SiO_2$) was prepared by the addition of the $NaAlO_2$ dan silica colloidal mixture into NaOH solution. The mixture was stirred continuously to form a homogeneous mixture and was left to age for 24 h at room temperature. The feedstock gel ($Al_2O_3.4.3SiO_2$) was also prepared following similar procedures but sodium aluminate was replaced by kaolin. The resulting feedstock gel was then added to the seed gel with the ratio of 18:1 in order to get overall synthesis gel mixture. The gel mixture was left to age for 24 h at room temperature before transferred into Teflon line vessel and hydrothermally treated at 105°C for 12h. The simplified synthesis process was illustrated in the schematic diagram in Fig.1.
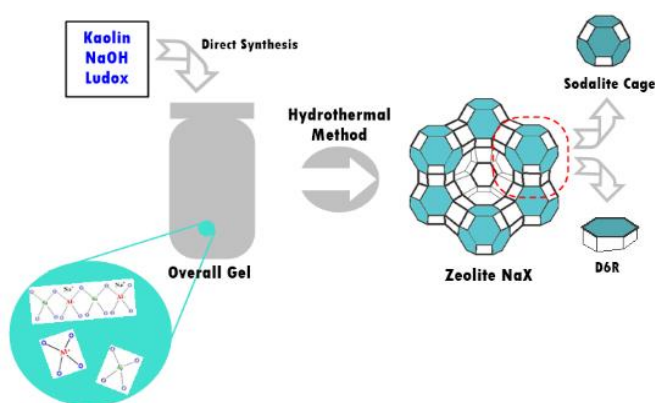

Fig. 1 The schematic diagram for the synthesis of zeolite NaX from kaolin.

The resulting powder was washed thoroughly with distilled water until the pH of the supernatant was neutral. The powder was then dried and calcined under an air flow at 500°C for 1h at 2°/min ramp rate. The synthesised zeolite NaX was ion-exchanged with NH_4^+ by mixing the resulting powder with ammonium acetate to form NH_4X, as shown in the following equation (1)(2).

$$NaX + CH_3COONH_4 \rightarrow NH_4X + CH_3COONa \qquad (1)$$

$$NH_4X \rightarrow HX + NH_3 \qquad (2)$$

The NH_4X was then calcined at 550°C for 5 hours to form H-zeolite X framework.

Characterization of synthesized zeolite NaX

X-ray Fluorescence was used to obtain chemical composition of Kaolin. The synthesized NaX powder and kaolin were also characterised using X-ray Diffraction (XRD) Philip Expert with CuKa (λ = 1.5405 Å) radiation to determine the crystalline phase and crystallinity. Data were recorded in the range of 5−40° with a step size of 0.02°. The infrared spectra of NaX (SiO_2/Al_2O_3 ratio = 4) was recorded using Fourier Transform Infrared spectrophotometer (8400S Shimadzu) with KBr pellet method. Sample and KBr were mixed with the ratio of 1:99, crushed and molded into a pellet, then compressed using hydraulic pressure. The formed pellet was placed on the holder and recorded in 4000-400 cm^{-1}.

The morphology of the synthesis zeolite X was analysed using *Scanning Electron Microscopy* (SEM) ZEIS EVO MA 10 FT-IR. Prior to the analysis, the sample was placed on a carbon tape and coated using Pd / Au for 15 minutes at 6 x 10^{-2} mBar pressure, then scanned to analyse the sample morphology.

Nitrogen adsorption-desorption isotherms were observed using the Quantachrome Corporation (Nova-1200) instrument. Prior to the analysis, 0.2 gram of sample was placed in the vacuum for 3 hours at

300 °C to evacuate adsorbed water, the sample was then exposed to nitrogen gas at 77 K. The specific surface area (S_{BET}) is calculated using BET (Brunauer-Emmet-Teller) equation. The total pore volume was obtained based on the amount of nitrogen adsorbed at P/P_o 0-0.99, while the pore size distribution was analyzed using BJH (Barret-Joiner-Halenda). The micropore size distribution was analysed using SF (Saito-Foley) method.

Pyridine was used as a probe molecule for acidity studies. The sample was weight ~10 mg and pressed to form a thin and transparent film. The film was then placed in the sealed sample holder and annealed in a tubular furnace under vacuum at 300 °C for 3 hours. The film was cooled at 30 °C before exposed with pyridine. The temperature was increased to 150 °C to remove physisorbed pyridine on the surface. The chemical adsorption of pyridine on the zeolite X was measured using FTIR and the adsorbed pyridine peak was determined using the Gaussian method.

RESULTS AND DISCUSSION

Characterisation of zeolite NaX

Detail chemical composition of kaolin obtained from XRF analysis was summarised in Table 1. Kaolin predominantly consisted of SiO_2 and Al_2O_3 at ~ 91 wt. % with the impurities consisted of K_2O, Fe_2O_3, and traces of metal oxides. Considering the low level of metal oxide impurities, kaolin was used without prior pre-treatment for the synthesis of zeolite X. We provide EDX analysis of the as-synthesised zeolite X that indicated the NaX consisted of siliconnium and oxygen as main elements for zeolite framework with sodium that presumably as stabilizer cation (Fig. 2). We imply that metal oxide impurities that were originally present in kaolin were successfully evacuated from the reaction mixture. The evacuation occurred during the dissolution of kaolin with sodium hydroxide followed by thorough washing with deionised water and air calcination at high temperature.

Table 1 Minerals analysis by XRF for Kaolin.

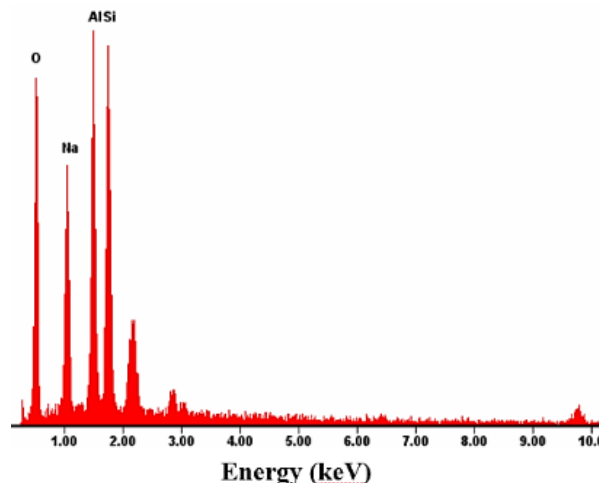| Minerals	Wt. %
Al_2O_3	36
SiO_2	54.9
P_2O_5	0.88
K_2O	2.88
CaO	0.58
TiO_2	0.551
V_2O_5	0.03
Fe_2O_3	3.37
CuO	0.097
Rb_2O	0.18
ZnO	0.02
NiO	0.585

Fig. 2 EDX analysis on the elemental composition of synthesized NaX

In order to synthesis zeolite NaX with high crystallinity and purity, the synthesis condition should be carefully controlled including the purity of the precursors. The hydrothermal treatment requires optimisation of synthesis condition by controlling the temperature and the crystallisation time. Variation of the molar ratio of starting materials significantly determined morphology, surface area and acidity of the synthesized zeolite. Davis [13] reported that controlling the temperature of hydrothermal treatment affected the nucleation and crystal growth of zeolite. In general, hydrothermal synthesis at high temperature produced high thermal energy that consequently shortened the crystallization time. However, synthesis at high temperature often produced large aggregates of zeolite. We found the optimum crystallization temperature for the synthesis of zeolite NaX from kaolin was achieved at 105 °C. Detail analysis of the morphological structure and the purity of the synthesized zeolite was analysed using XRD and infrared spectroscopy.

X-ray diffractogram of kaolin, synthesised zeolite NaX and commercial zeolite NaX were shown in Fig 3. The peaks corresponded to kaolin at 20º, 20.5º, 22º, 35º, 36º, 39º and 40º were significantly reduced in the as-synthesised zeolite NaX. The diffractogram pattern of zeolite NaX synthesised using kaolin showed peaks at $2\theta = 6.15; 10.02; 23.28; 26.64; 31.95°$ which were identical to the peaks appeared in standard zeolite X [13]. The XRD pattern of synthesized zeolite NaX was also in accordance with the peaks of NaX according to International Zeolite Association (IZA)[14]. However, two peaks corresponded to kaolin at 13º and 25º were still present but at significantly low intensity in zeolite NaX which suggested incomplete dissolution of kaolin with sodium hydroxide during the preparation of gel mixture.
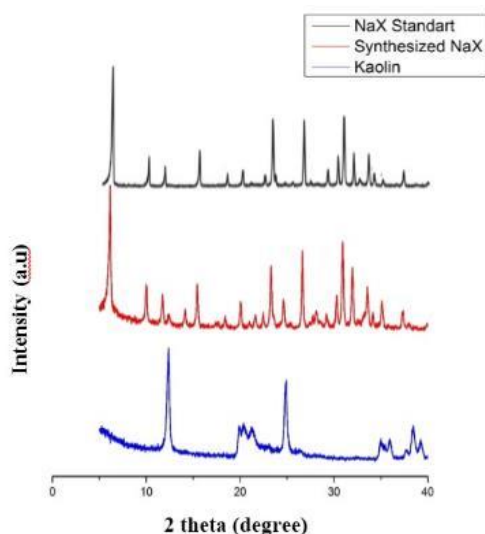

Fig. 3 The XRD pattern of NaX commercial standard, synthesize NaX and kaolin.

The synthesized zeolite NaX was also analysed using infrared spectroscopy to provide spectroscopic evidence on the structure and the functional group of zeolite X. The IR spectra of zeolite X was also compared to kaolin as shown in Fig.4. The presence of a band at 1107 cm^{-1} in the infrared analysis of kaolin indicated the stretching vibration of tetrahedral SiO_4 and AlO_4. The peak appeared at 1029 cm^{-1} is corresponded to the vibration of Si-O-Si (Si-O-Si in-plane stretching). The vibration of Al-O-H appeared at 913 cm^{-1} which subsequently disappeared in NaX spectra. The characteristic bands of NaX which consisted of FAU type structure occurred between 1250-950 cm^{-1}[15] which showed external asymmetric stretching of TO_4, where T is Si or Al. The band appeared at 790-650 cm^{-1} is external vibration associated with the sensitive tetrahedral structure of zeolite X (external symmetric vibration). This is a typical vibration that appears in most silica materials [16]. Asymmetric stretching and symmetric stretching of synthesized NaX can be seen occurred at 977.94 cm^{-1} and 744.55 cm^{-1}. The specific TO_4 (T = Si or Al) vibrational peak for zeolite was identified by band appeared at 451 cm^{-1}. The peak observed at 561 cm^{-}

[1] was identified as vibrational of D6R rings that distinguished zeolite X structure with another aluminosilicate zeolite. The spectroscopic evidence obtained from the infrared analysis further consolidate the formation of zeolite X crystal structure that was synthesised using that kaolin as silica and alumina precursor.
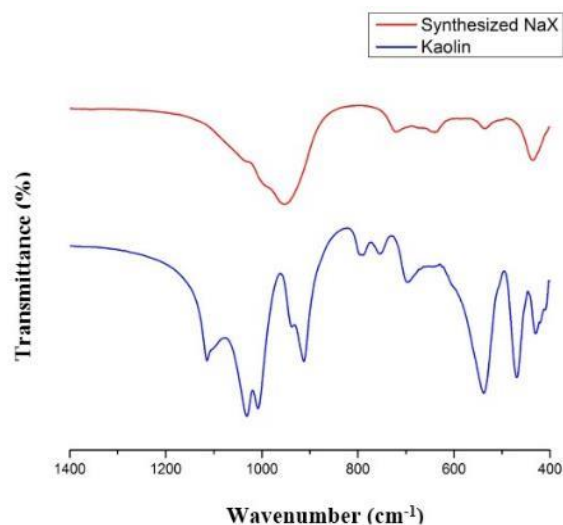

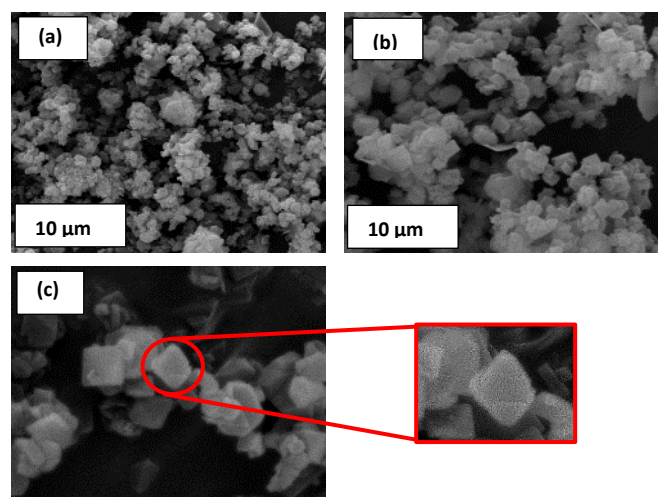**Fig. 4** The Spectra FTIR of synthesized NaX and kaolin.

Fig. 5 The SEM micrograph of synthesized NaX.

The morphology and crystallite size of the synthesised material was analysed using Scanning Electron Microscopy (SEM). Fig. 5 shows the morphology of NaX which appears as a hexagonal structure with average crystallite size ~ 10-20 µm. This is a typical morphology for zeolite X which were observed previously by others [17] [18]. SEM images also show the NaX crystallite was in uniform aggregate size and some crystallite agglomerates to form large aggregates. The presence of remaining kaolin as a result of incomplete dissolution which was indicated by XRD analysis was observed as a thin layer occurs around the NaX crystallite. The incomplete dissolution of kaolin also affected the Si/Al ratios of the synthesised zeolite X. The EDX analysis shown Fig.2 indicated that the zeolite X was consisted of 23 wt % of Si and 18 % of Al to give the Si/Al ratio of 1.28. This is significantly lower than the experimental value which also suggested incomplete dissolution of kaolin during the synthesis.

The specific surface area of kaolin and zeolite X were analysed using BET method with the nitrogen adsorption-desorption profile provides information on the type of pore of zeolite (Fig. 6). Kaolin showed no nitrogen adsorption at relative pressure, P/P_o within 0.1-0.3 which indicated the type II non-porous material. The non-porous kaolin also has a very low surface area of ~ 14 m^2/g. The transformation of

kaolin to zeolite X resulting in a high surface area (80 m^2/g) material that is beneficial for research and industrial purposes. The as-synthesised zeolite HX showed an isotherm type IV which indicated the presence of mesoporous structure within the framework.
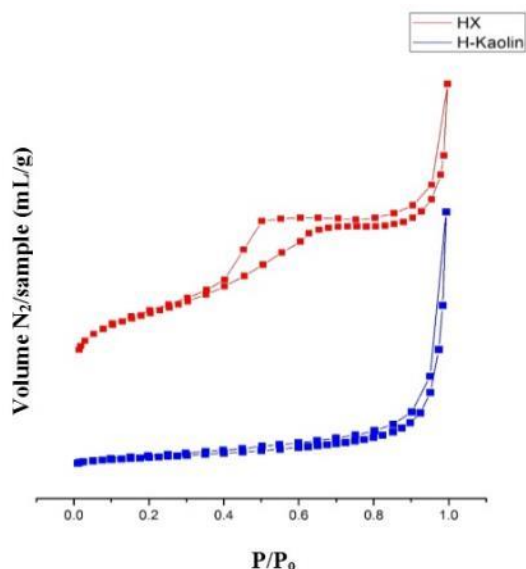

Fig. 6 The Isotherm N$_2$ Adsorption-Desorption of HX and H-kaolin.

The isotherm N$_2$ profile of HX exhibited an increasing nitrogen molecule adsorption at low relative pressure (0 to 0.3) corresponding to the adsorption occurred to fill the micropores of zeolite. At P/P$_o$ of 0.3, the surface of zeolite X was covered by a monolayer nitrogen molecule. Adsorption of nitrogen to the zeolite surface was continuously increased at P/P$_o$ ~ 0.4-0.7, which indicated the nitrogen adsorption on the uniform slit-shaped intracrystal mesopore. The surface of the pore only allowed a limited layer of adsorbate, its called condensation and causing the hysteresis loop. Hysteresis loop was observed at P/P$_o$ 0.4-1, occurred due to the desorption of nitrogen.
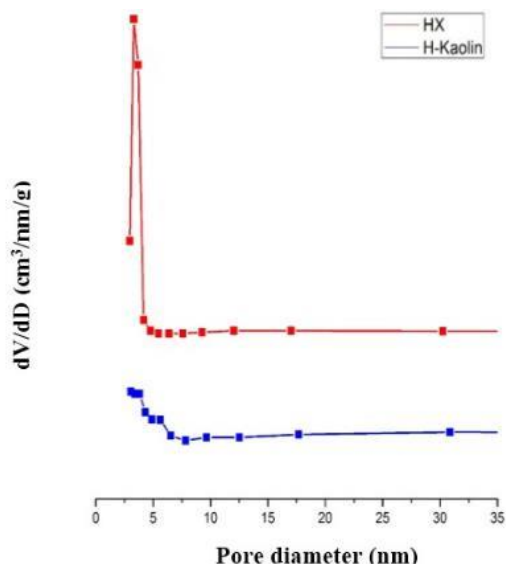

Fig. 7 The pore size distribution of kaolin and synthesized HX from BJH (Ballet, Joiner, Halenda) method.

Analysis of the pore size distribution using the BJH (Barret, Joiner, Halenda) method in Fig. 7 showed the presence of meso-sized pore type structure ~ 2-5 nm in diameter with a peak centered at 3.4 nm. It implies that the zeolite NaX consisted of the intra-crystal mesoporous structure with narrow and sharp pore distribution. We also compare the pore size distribution of zeolite NaX with the raw material kaolin that showed no significant pore structure can be observed in kaolin. This is in

agreement with the N$_2$ adsorption-desorption analysis that revealed type II isotherm corresponded to the non-porous structure of kaolin. The formation of mesopores within the zeolite NaX structure is rather surprising due to in general the synthesis of mesoporous zeolite requires the presence of surfactant as structure directing agent. We suggested the formation of mesoporous structure is due to the arrangement of silica and alumina in the slit-pore of zeolite NaX. Apart from the presence of mesopores, analysis of zeolite NaX SF method as shown in Fig. 8 also indicated the presence of the microporous structure. The micropore size distribution showed the highest pore diameter of ~ 1.47 nm with a micropore volume of ~ 0.006 cm^3/g contrary to kaolin that only consisted of relatively small micropore size within 0.36 and 0.90 nm of diameter.

The surface acidity was performed by infrared spectroscopy using pyridine as a probe molecule. The amount of adsorbed pyridine on the zeolite NaX was analysed in the 1700-1400 cm^{-1} of wavelength region. Protonated pyridine molecule in the form of pyridium ion (C$_5$H$_5$NH$^+$) interacting with Brønsted acid sites shows a specific adsorption band at a wavenumber of ~ 1540-1545 cm^{-1}. The pyridinium ion is a result of bond formation between pyridine with a proton from the surface hydroxyl group of zeolite X. Interaction between pyridine with Lewis acid site on the surface formed by coordinated bonding interaction between the free electron pairs of pyridine molecule with the empty orbital of extra -framework alumina in the zeolite. This interaction leads to the appearance of the absorption band at wavenumber ~1440-1452 cm^{-1} [19].
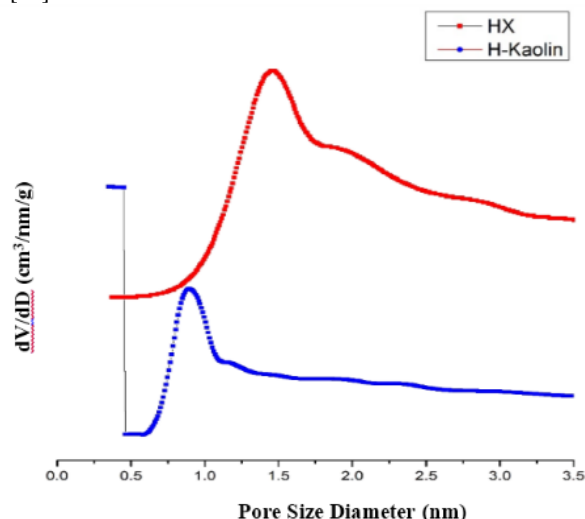

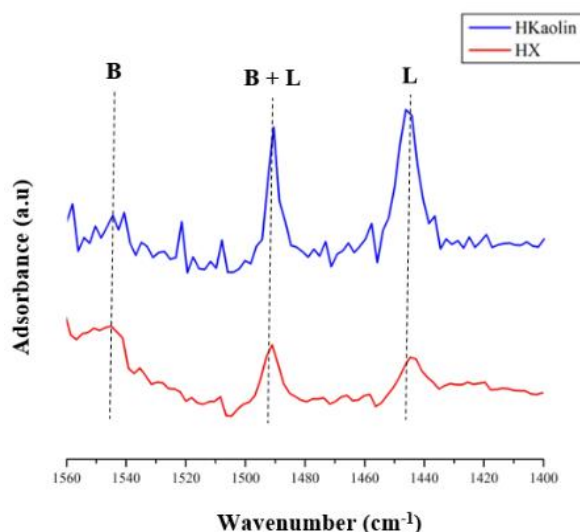**Fig. 8** The micropore distribution of as-synthesized HX from the SF method

Fig. 9 The infrared spectra of pyridine adsorption of synthesized HX

The infrared spectra of the pyridine upon adsorption on zeolite HX showed pyridine peak vibration appeared ~ 1440-1452 cm^{-1} indicating the presence of Lewis acidity. The band appeared at 1545 cm^{-1} revealed Brønsted acidity and the band at 1490 cm^{-1} corresponded to the total adsorption of pyridine on both Lewis and Brønsted acid sites [20]. The peak area of adsorbed pyridine was determined using the Gaussian method to indicate the amount of surface acid site on the as-synthesised zeolite X. The calculated data showed the zeolite X has a high number of Brønsted acidity in comparison to Lewis acidity to give about ~0.18 mmol/g of the Brønsted acid site and 0.05 mmol/g of Lewis acid site.

CONCLUSION

We investigated the potential use of abundantly available silica and alumina riched kaolin to be transformed into zeolite X. The synthesis occurs in three steps involving the preparation of seed gel, the formation of feedstock gel using kaolin and the mixture of these two gels to form the overall gel. The crystallization process was carried out under a hydrothermal condition at 105°C which produced zeolite NaX with both microporous and mesoporous structure. The zeolite NaX also consisted of high purity and crystallinity with high surface acidity which ideal as a catalyst in many catalytic applications.

ACKNOWLEDGEMENT

REFERENCES

[1] S. Chandrasekhar, P.N. Pramada, Investigation on Synthesis of Zeolite NaX from Kerala Kaolin, *Journal of Porous Materials* (2004) 6:283-297.

[2] Y. Liu, C. Yan, X. Qiu, D. Li, H. Wang, A.Alshameri, Preparation of Faujasite Block from Fly Ash-Based Geopolymer via in-Situ Hydrothermal Method, *Journal of the Taiwan Institute of Chemical Engineers* 433–39 (2016) 59.

[3] R.M. Mohamed, I.A. Mkhalid, M.A. Barakat, Rice husk ash as a renewable source for the production of zeolite NaY and its characterization, *Arabian Journal of Chemistry* 48-53 (2012) 8.

[4] J.-Q.Wang, Y.-X. Huang, Y. Pan, Hydrothermal Synthesis of High Purity Zeolite A and X from Natural Kaolin without Calcination *Microporous and Mesoporous Materials* 50–56 (2014) 199.

[5] C. Belviso, F. Cavalcante, A. Lettino, S. Fiore, A and X-Type Zeolites Synthesised from Kaolinite at Low Temperature, *Applied Clay Science* 162–68 (2013) 80-81.

[6] J-Q. Wang, Y. Pan, New Hydrothermal Route for the Synthesis of High Purity Nanoparticles of Zeolite X from Kaolin and Quartz, *Microporous and Mesoporous Material* 77–85 (2016) 232.

[7] Y. Ma, C. Yan, A. Alshameri, X. Qiu, D. Li, C. Zhou, Synthesis and Characterization of 13X Zeolite from Low-Grade Natural Kaolin, *Advanced Powder Technology* 495–99 (2014) 25.

[8] V. Garshasbi, M. Jahangiri, M. Anbia, Equilibrium CO2 Adsorption on Zeolite 13X Prepared from Natural Clays, *Applied Surface Science* 225–33 (2017) 393.

[9] K.-H.Chung, D.-R. Chang, B.-G. Park, Removal of Free Fatty Acid in Waste Frying Oil by Esterification with Methanol on Zeolite Catalysts, *Bioresource Technology* 38–43 (2008) 99.

[10] K.M. Roghayeh, S.A. Fakhry, Study on the Thermal Behavior of Low Silica X-type Zeolite Ion Exchanged with Alkaline earth Cation, *Microporous and Mesoporous Material* 285-293 (2009) 120.

[11] Z. Xu, T. DaQing, Z. JingJing, L. XingYang, Synthesis of NaX Zeolite at Room Temperature and Its Characterization, *Material Letters* 80-83 (2013) 104.

[12] W. Jin-Quan, H. Ya-Xi, P. Yuanming, X. Jin, Hydrothermal Synthesis of High Purity Zeolite A from Natural Kaolin without Calcination, *Microporous and Mesoporous Material 50-56 (2014) 199.*

[13] M. Davis, Zeolite and Molecular Sieve Synthesis, *Chemistry Material* 756-768 (1992) 4.

[14] C.W.Purnomo, C.Salim, H. Hinode, Synthesis of Pure Na–X and Na–A Zeolite from Bagasse Fly Ash, *Microporous and Mesoporous Materials*, 6–13 (2012) 162.

[15] W. Mozgawa, M. Krol, Barczyk, FTIR Studies of Zeolites from Different Structural Groups, *CHEMIK* 667-674 (2011) 65.

[16] D. Chen, X. Hu, L. Shi, Q. Cui, H. Wang, H. Yao, Synthesis and Characterization of Zeolite X from Lithium Slag, *Applied Clay Science* 148–51 (2012) 59-60.

[17] J.M. Gómez, E. Diez, I. Bernabé, Deoxygenation of M-Toluic Acid over Hierarchical X Zeolite, *Catalysis Communications* 55–58 (2016) 78.

[18] H.J. Lee, Y.M. Kim, O.S.Kweon, I.J. Kim, Structural and Morphological Transformation of NaX Zeolite Crystals at High Temperature, *Journal of the European Ceramic Society* 561–64 (2007) 27.

[19] K.A. Layman, M.M. Ivey, J.C. Hiemminger, Pyridin Adsorption and Acid/Base Complex Formation on Ultrathin Films of γ-Al$_2$O$_3$ on NiAl (100), *Journal Physic Chemistry* 8538–8546 (2003) 107.

[20] S.Bendenia, I. Batonneu-Gener, J. Camparot, K. Marouf Khelifa, H. Hammoudi, A. Khelifa, Acidity Study of X Zeolites Modified by Nickel And/or Chromium Cations in the Case of Binary and Ternary Exchanges, *Microporous and Mesoporous Materials* 111–18 (2012) 159.